

Error Performance Analysis in Downlink Cellular Networks with Interference Management

Laila Hesham Afify[§], Hesham ElSawy[§], Tareq Y. Al-Naffouri^{§*}, and Mohamed-Slim Alouini[§]

[§] King Abdullah University of Science and Technology (KAUST), Thuwal, Makkah Province, Saudi Arabia.

* King Fahd University of Petroleum and Minerals (KFUPM), Dhahran, Saudi Arabia.

Email: {laila.afify, hesham.elsawy, tareq.alnaffouri, slim.alouini}@kaust.edu.sa

Abstract—Modeling aggregate network interference in cellular networks has recently gained immense attention both in academia and industry. While stochastic geometry based models have succeeded to account for the cellular network geometry, they mostly abstract many important wireless communication system aspects (e.g., modulation techniques, signal recovery techniques). Recently, a novel stochastic geometry model, based on the Equivalent-in-Distribution (EiD) approach, succeeded to capture the aforementioned communication system aspects and extend the analysis to averaged error performance, however, on the expense of increasing the modeling complexity. Inspired by the EiD approach, the analysis developed in [1] takes into consideration the key system parameters, while providing a simple tractable analysis. In this paper, we extend this framework to study the effect of different interference management techniques in downlink cellular network. The accuracy of the proposed analysis is verified via Monte Carlo simulations.

Keywords—Cellular networks, equivalent-in-distribution, interference management, stochastic geometry, symbol error probability.

I. INTRODUCTION

Due to the exponential growth of the emerging wireless applications, wireless networks inevitably suffer from concurrent transmissions which significantly affect their performance. Statistical characterization of the resulting interference has drawn the attention of several research attempts. However, in order to study the inter-cell interference behavior, it is essential to account for the impact of various random factors on the interfering links. Specifically, in cellular networks, base stations (BSs) locations were found to exhibit random patterns rather than the deterministic grids [2]–[5]. The imposed random network topology introduces numerous uncertainties to the system model, which renders modeling and understanding the aggregate network interference a complex and challenging task. To this end, tools from stochastic geometry have been exploited to model and analyze interference in such networks. One common approach to characterize the aggregate network interference is to account for the coherent sum of interfering signal powers at a test receiver [2]–[4], [6]. This approach has been found accurate and useful in modeling outage probability, defined as the probability that the signal-to-interference-and-noise-ratio (SINR) goes below a certain threshold, and ergodic rate, defined by Shannon capacity formula.

For example, in [3] the SINR coverage probability (the complement of outage) and rate in multi-tier saturated downlink cellular networks have been investigated. A load-aware extension of [3] is presented in [7]. Ergodic rate and outage

in multi-tier uplink cellular networks with channel inversion power control are modeled in [6]. The performance of uplink cellular network with fractional channel inversion power control is presented in [8]. Cognitive cellular networks performance is analyzed in [9]. The work in [10] derives the asymptotic spectral efficiency for uplink multi-antenna cellular networks. The authors in [11] provide a general framework that captures the performance of downlink MIMO HetNets in terms of coverage probability, per user rates, and area spectral efficiency for different MIMO setups. In [12], the exact coverage probability in downlink MIMO HetNets under flexible cell association has been developed. In the context of interference management, [13] provides a tractable analysis for successive interference cancellation (SIC) in downlink OFDM-based heterogeneous cellular networks. In [14], the authors investigate the improvement in coverage under BSs coordinated multi-point transmission (CoMP) in the downlink communication. Moreover, in [15] the performance in a location-aware two-tier CoMP scheme has been quantified.

SINR characterization via its cumulative distribution function (CDF), i.e., outage probability, is a common factor in the aforementioned literature. It is worth mentioning here that the SINR threshold, used to define outage, is chosen arbitrarily and does not provide a clear understanding for the network performance. Additionally, dealing with interference as the coherent sum of powers limits the analysis and overlooks the effect of several fundamental system aspects (e.g., modulation scheme, constellation type, and signal recovery techniques). Therefore, it is essential to complement these efforts and study tangible and more meaningful performance metrics, beyond coverage probability and rates, that capture the key network features such as spatially averaged error rates.

Error rate performance analysis has mainly been studied for AWGN or Gaussian interference channels [16, chapter 8], which is not the case in cellular networks. Hence, the available expressions for error rate does not apply to the cellular network case. To avoid this problem, the authors in [17] extended the conditionally Gaussian representation for Poisson field of interference proposed [18] to cellular networks. This representation renders all AWGN error rate expressions legitimate to be used, in cellular networks, to obtain conditional error performance. The obtained ASEP expressions are then deconditioned to obtain the de facto error performance. The model proposed in [17], referred to as the *Equivalent-in-Distribution* (EiD) approach, treats the aggregate interference as the noncoherent superposition of the interfering signals and captures the modulation scheme, constellation type, and signal recovery method into the analysis. Applying this framework, the average bit error probability

(ABEP) and average error symbol probability (ASEP) can be characterized in cellular networks. Although the EiD approach provides an accurate representation for realistic interference, it yields complex analysis for the ASEP performance evaluation. Another approach in [1], which is inspired by the work in [17]–[19], approximated the interfering symbols with Gaussian codebooks to represent the distribution of the out-of-cell aggregate interference signal by a conditionally Gaussian distribution, when conditioning on the network geometry. Hence, the ASEP expressions for AWGN channels are legitimate to be exploited. It has been shown that the proposed analysis in [1] circumvents the complexity of the EiD approach by abstracting unnecessary system details (i.e., the interferers transmitted symbols) without compromising the performance accuracy.

In this work, we take advantage of the unified framework developed in [1], to quantify the effect of interference management on the ASEP performance in downlink cellular systems. It is to be noted that both the EiD and the proposed analysis rely on the conditionally Gaussian interference representation, however, the presented analysis yields simple single-integral ASEP expressions even in Nakagami fading environment, unlike the EiD approach which results in a computationally intensive double-integral expressions [17, equation (10)].

II. SYSTEM MODEL

We consider a single-tier cellular network where the distribution of the BSs is modeled via a homogeneous PPP, denoted as $\Psi_B = \{x_i, i = 0, 1, 2, \dots\}$, with intensity λ . Extension to multi-tier case is straightforward following the framework in [3]. The locations of the UEs follow a stationary point process Ψ_u . According to Slivinyak's Theorem [20], there is no loss in generality to focus on the performance of a user located at the origin and assume that the elements in Ψ_B are ordered w.r.t. their locations from the origin. Hence, we have $\|x_o\| < \|x_1\| < \|x_2\| < \dots$, where $\|\cdot\|$ is the Euclidean norm. Each of the BSs and the UEs is equipped with a single antenna. Saturation conditions are assumed such that all BSs will always have users to serve. All BSs transmit with a constant power P in the downlink and radio signal strength based association is adopted, hence the test user is associated to the BS located at x_o . Under the aforementioned association methodology, it is easy to show that the distance between a typical user and its serving BS, denoted by $\|x_o\|$, has the following Rayleigh distribution [20]

$$f_{\|x_o\|}(x) = 2\pi\lambda x \exp\{-\lambda\pi x^2\}, \quad x > 0 \quad (1)$$

Let η and denote an environment-dependent path-loss exponent. We assume an unbounded path-loss model where the transmitted signal power decays at the rate $r^{-\eta}$ with the distance r . In addition to the distance decay, signals also experience unit mean (i.i.d.) Nakagami- m channel power gains, where m is assumed to be an integer. Therefore, the analysis is valid for various fading environments, as Nakagami- m can approximate several fading models. The core part of the paper considers a baseline network model with universal frequency reuse scheme. Then, for the purpose of interference management, BSs coordination and frequency reuse are considered. Note that, traditional hexagonal grid tailored frequency reuse schemes cannot be employed due to the random network structure. Instead, the available spectrum

is divided into Δ sub-bands and each BS selects one of the sub-bands for transmission. We analyze two sub-band selection schemes, namely, random frequency reuse and coordinated frequency reuse schemes. In the random frequency reuse scheme, each BS selects one of the Δ sub-bands with equal probability. On the other hand, the coordinated frequency reuse scheme necessitates that the BSs coordinate together such that the Δ -closest neighboring BS use different frequencies¹.

At the BS side, data is mapped to a general bi-dimensional unit-power constellation \mathbf{S} with \mathcal{K} equiprobable symbols denoted by $s^{(\kappa)}$, $\kappa = 1, 2, \dots, \mathcal{K}$, such that, $\mathbb{E}[|s^{(\kappa)}|^2] = 1$. However, since we are only interested in our test receiver performance, we abstract other interferers transmission by Gaussian signals s_i with unit power spectral density². Note that this is the core assumption that discriminates the proposed analysis from the EiD approach, which statistically accounts for the actual transmitted symbols from each interferer [17].

At the test UE side, the intended symbol is recovered via a Maximum-likelihood receiver (MLR) with perfect Channel State Information (CSI). Furthermore, it is assumed that the test receiver has perfect intended link CSI and is unaware of the inter-cell interference. The complex signal received at the test user for the downlink scenario can be written as

$$y = \sqrt{P}g_o s_o \|x_o\|^{-b} + \sum_{x_i \in \tilde{\Psi} \setminus x_o} \sqrt{P}g_i s_i \|x_i\|^{-b} + n, \quad (2)$$

where $\tilde{\Psi}$ is the set of interfering BSs that depends on the employed frequency reuse scheme, e.g., $\tilde{\Psi} = \Psi_B \setminus x_o$ in the case of universal frequency reuse. g_o and g_i are independent unit mean gamma random variables representing the intended and interfering channel gains in a Nakagami-fading environment, with parameters m_o and m , respectively. Finally, $b = \frac{\eta}{2}$, and $n \sim \mathcal{CN}(0, N_o)$ denotes the circularly symmetric complex Gaussian noise at the receiver.

III. PROPOSED ASEP ANALYSIS

In this section, we first introduce the baseline general ASEP framework with no interference management or frequency reuse. Then, in the next section, we build on these results to analyze the BS coordination and/or frequency reuse.

A. Baseline Model

Due to the Gaussian codebook assumption for the interfering signals (i.e., $s_i \sim \mathcal{CN}(0, 1)$), the aggregate interference in (2) is conditionally Gaussian (i.e., conditioned on $\|x_o\|$, g_i and $\|x_i\| \forall i$). Hence, the conditionally averaged SINR can be represented as

$$\begin{aligned} \Upsilon(g_o, \|x_o\|, g_i, \|x_i\|) &= \frac{(\mathbb{E}[y|g_o, \|x_o\|, g_i, \|x_i\|])^2}{\text{Var}(y|g_o, \|x_o\|, g_i, \|x_i\|)} \\ &= \frac{P \|x_o\|^{-\eta} g_o}{\sum_{x_i \in \Psi_B \setminus x_o} P g_i \|x_i\|^{-\eta} + N_o} \\ &= \frac{g_o}{\sum_i \text{SIR}_i^{-1} + \text{SNR}^{-1}}, \end{aligned} \quad (3)$$

¹The Δ -closest BSs are with respect to the UE not the BS.

²This assumption is only reflected in our analysis, in the simulation and EiD results, all interferers follow the same modulation scheme as the test transmitter.

where $\text{SIR}_i = \frac{\|x_o\|^{-\eta}}{g_i \|x_i\|^{-\eta}}$ is the average received signal-to- i^{th} interference-ratio, while $\text{SNR} = \frac{P\|x_o\|^{-\eta}}{N_o}$ is the average received signal-to-noise-ratio.

Since Υ is averaged over a zero-mean conditionally Gaussian aggregate interference signal, we can utilize the ASEP expressions for AWGN channels in fading environments. Then, we can average over $g_o, \|x_o\|, g_i,$ and $\|x_i\|$ to obtain the de facto ASEP performance. For any modulation scheme \mathcal{M} , the ASEP for the MLR in AWGN channels can be expressed in the form

$$\text{ASEP}(\mathcal{M}|\Upsilon) = \sum_{j=1}^{\kappa(\mathcal{M})} w_j \int_0^{\mu_j} e^{-\Upsilon \frac{\beta_j}{\sin^2 \vartheta}} d\vartheta, \quad (4)$$

where $\kappa(\mathcal{M})$ is the number of terms that constitute the ASEP expression for the modulation scheme \mathcal{M} , w_j is a modulation-dependent weighting factor, and μ_j and β_j are modulation-specific parameters. In this paper, we focus on square quadrature amplitude modulation scheme, i.e., M -QAM. Re-writing (4) in terms of the complementary error function $\text{erfc}(x) = \frac{2}{\sqrt{\pi}} \int_x^\infty e^{-t^2} dt$ [22], and following [16, chapter 8], we yield the ASEP conditioned on the SINR as

$$\text{ASEP}(M\text{-QAM}|\Upsilon) = w_1 \text{erfc}(\sqrt{\beta\Upsilon}) + w_2 \text{erfc}^2(\sqrt{\beta\Upsilon}), \quad (5)$$

where $w_1 = 2\sqrt{\frac{M-1}{M}}$, $w_2 = -\left(\frac{\sqrt{M-1}}{\sqrt{M}}\right)^2$, and $\beta = \frac{3}{2(M-1)}$. As mentioned earlier, the de facto ASEP is obtained by deconditioning on $(\|x_o\|, g_i, \|x_i\|)$.

The averaging step is challenging because it requires the knowledge of the probability density function (PDF) of the SINR, which is not available. This is owing to the fact that there are no explicit expressions for the interference PDF even for the simple PPP, except for very special cases which are not valid for cellular networks [5]. However, we can still overcome this problem by exploiting the results in [21], which enable us to express the quantities $\mathbb{E}[\text{erfc}(\sqrt{\Upsilon})]$ and $\mathbb{E}[\text{erfc}^2(\sqrt{\Upsilon})]$ in terms of the LT of the interference power. In [21], the authors proposed a technique to calculate averages in the form of $\mathbb{E}[\text{erfc}(\sqrt{\frac{Y}{X+C}})]$ and $\mathbb{E}[\text{erfc}^2(\sqrt{\frac{Y}{X+C}})]$ such that Y is a gamma random variable with unity mean, C is a constant, and X is considered to have an arbitrary distribution with LT $\mathcal{L}_X(\cdot)$. These averages are given by

$$\mathbb{E}\left[\text{erfc}\left(\sqrt{\frac{Y}{X+C}}\right)\right] = 1 - \frac{\Gamma(m_o + \frac{1}{2})}{\Gamma(m_o)} \frac{2}{\pi} \int_0^\infty \frac{1}{\sqrt{z}} e^{-z(1+m_o C)} {}_1F_1\left(1 - m_o; \frac{3}{2}; z\right) \mathcal{L}_X(m_o z) dz, \quad (6)$$

and

$$\mathbb{E}\left[\text{erfc}^2\left(\sqrt{\frac{Y}{X+C}}\right)\right] = 1 - \frac{4\Gamma(m_o + 1)}{\pi} \int_0^\infty e^{-zm_o C} \mathcal{L}_X(m_o z) \int_0^{\frac{\pi}{4}} {}_1F_1\left(m_o + 1; 2; \frac{-z}{\sin^2 \vartheta}\right) \frac{d\vartheta}{\sin^2 \vartheta} dz, \quad (7)$$

such that $\Gamma(x) = \int_0^\infty t^{x-1} e^{-t} dt$ is the Gamma function, ${}_1F_1(a; b; z) = \sum_{k=0}^\infty \frac{(a)_k}{(b)_k k!} z^k$ is the Kummer confluent hypergeometric function with $(a)_q = \frac{\Gamma(a+q)}{\Gamma(a)}$ as the Pochhammer symbol [22].

Projecting back to the SINR expressions in (5), $Y = g_o$, $X = \sum_i \text{SIR}_i^{-1}$ and $C = \text{SNR}^{-1}$ which is a constant when conditioning on $\|x_o\|$. Next, it is essential to characterize the LT of $\sum_i \text{SIR}_i^{-1}$, in order to use the aforementioned expressions. The LT of $X = \sum_i \text{SIR}_i^{-1}$ is given by [1]

$$\begin{aligned} \mathcal{L}_X|_{\|x_o\|}(s) &= \mathbb{E}\left[e^{-s \sum_{i \in \Psi_B} \frac{\|x_i\|^{-\eta} g_i}{\|x_o\|^{-\eta}}}\right] \\ &= \exp\left\{-\pi\lambda \|x_o\|^2 \left[{}_2F_1\left(\frac{-2}{\eta}, m; 1 - \frac{2}{\eta}; \frac{-s}{m}\right) - 1\right]\right\}. \end{aligned} \quad (8)$$

Accordingly, the ASEP for the downlink communication links is provided by Theorem 1, given at the top of the next page, which is obtained by plugging (6), (7), and (8) into (5).

B. Interference Management

In this section, we study the ASEP performance under inter-cell interference management. As mentioned before, we consider two main frequency reuse schemes with Δ sub-bands. In the first, denoted as coordinated frequency reuse scheme, each BS chooses a sub-band not used by its $(\Delta - 1)$ neighboring BSs. In the second, denoted as random frequency reuse scheme, each BS randomly and independently chooses one of the sub-bands with probability $\frac{1}{\Delta}$. For the sake of comparison, we study BS coordination without frequency reuse, in which the test BS avoids or cancels the interference from the $(\Delta - 1)$ neighboring BSs only.

The random frequency reuse scheme is easy to incorporate into the analysis due to the independent and random selection of the frequency sub-band. As shown in [2], in the random frequency reuse scheme, the interfering BSs will constitute a PPP thinned by the factor Δ^{-1} . As a consequence, the LT of the interference is similar to (8) but with the intensity $\frac{\lambda}{\Delta}$. On the other hand, the analysis of the coordinated frequency reuse scheme is more involved for two reasons. The first is that the sub-band selection scheme introduces correlations, in the form of repulsion, between the set of BSs using the same frequency. Hence, the set of interfering BSs $\tilde{\Psi}$ is not PPP. The second, we have to find the joint distribution between the distance to the serving BS and the distance to the $\Delta^{\text{th}} - 1$ neighbor to estimate the interference protection imposed by the BS coordination. The conditional and joint distributions between the distance to the serving BS $\|x_o\|$ and the distance to the n^{th} neighboring BS are given the following lemma.

Lemma 1: The conditional PDF of the distance between a user, located $\|x_o\|$ away from its serving BS, to the n^{th} neighbor interfering BS is given by

$$f_{\|x_n\||\|x_o\|}(r|\|x_o\| = r_o) = \frac{2(\pi\lambda)^n r (r^2 - r_o^2)^{n-1} e^{-\pi\lambda(r^2 - r_o^2)}}{\Gamma(n)}, \quad (10)$$

where $r_o < r < \infty$. The joint PDF of $\|x_n\|$ and $\|x_o\|$ is given as

$$f_{\|x_n\|, \|x_o\|}(r, x) = \frac{4(\pi\lambda)^{n+1} x r (r^2 - r_o^2)^{n-1} e^{-\pi\lambda r^2}}{\Gamma(n)}, \quad (11)$$

Theorem 1: For the depicted system model, the ASEP expression in Nakagami- m fading environment for M -QAM modulated signals in the downlink with no interference management can be written as

$$\begin{aligned} ASEP = & w_1 \left(1 - \frac{\Gamma(m_o + \frac{1}{2})}{\Gamma(m_o)} \frac{2}{\pi} \int_0^\infty \exp \left\{ -\pi \lambda \|x_o\|^2 \left[{}_2F_1 \left(\frac{-2}{\eta}, m; 1 - \frac{2}{\eta}; \frac{-m_o z}{m} \right) - 1 \right] - z(1 + m_o C) \right\} \frac{1}{\sqrt{z}} {}_1F_1 \left(1 - m_o; \frac{3}{2}; z \right) dz \right) \\ & + w_2 \left(1 - \frac{4\Gamma(m_o + 1)}{\pi} \int_0^\infty \exp \left\{ -\pi \lambda \|x_o\|^2 \left[{}_2F_1 \left(\frac{-2}{\eta}, m; 1 - \frac{2}{\eta}; \frac{-m_o z}{m} \right) - 1 \right] - z m_o C \right\} \int_0^{\frac{\pi}{4}} {}_1F_1 \left(m_o + 1; 2; \frac{-z}{\sin^2 \vartheta} \right) \frac{d\vartheta}{\sin^2 \vartheta} dz \right). \end{aligned} \quad (9)$$

where $x < r < \infty$, where $0 \leq x \leq \infty$.

Proof: See Appendix A. \blacksquare

For the sake of simple presentation, we focus on the special case of $\eta = 4$ and Rayleigh fading with $m = m_o = 1$ in the rest of the paper. For analytical tractability, we approximate the set of interfering BSs, in the coordinated frequency reuse scheme, with a PPP with intensity $\frac{\lambda}{\Delta}$. It is well perceived that approximating a point process with repletion with an equidense PPP gives an accurate estimate for the interference if the exclusion distance around the test receiver is well estimated [5], [6], [9], [23], [24]. Exploiting the equi-dense PPP approximation and the interference exclusion distance estimated in Lemma 1, the LT of $X = \sum_i \text{SIR}_i^{-1}$ in the case of coordinated frequency reuse scheme is given by the following lemma.

Lemma 2: Let \mathcal{I}_Δ be the set of dominant interferers up to the nearest $\Delta^{th} - 1$ interferer. Thus, conditioned on $\|x_o\|$, the LT of \tilde{X} such that $\mathcal{L}_{\tilde{X}}(s) = \mathcal{L}_{X|\|x_o\|}(s)$ is written as (12).

Proof: See Appendix B. \blacksquare

As a result, conditioned on $\|x_o\|$, the ASEP is written as

$$\begin{aligned} A\hat{S}EP_{\text{IM}} = & w_1 \left(1 - \mathbb{E} \left[\int_0^\infty \mathcal{L}_{\tilde{X}|\|x_o\|} \left(\frac{z}{\beta} \right) \frac{e^{-z(1+\frac{c}{\beta})}}{\sqrt{\pi z}} dz \right] \right) \\ & + w_2 \left(1 - \frac{2}{\sqrt{\pi}} \mathbb{E} \left[\int_0^\infty \mathcal{L}_{\tilde{X}|\|x_o\|} \left(\frac{z}{\beta} \right) \frac{e^{-z(1+\frac{c}{\beta})}}{\sqrt{z}} \text{erfc}(\sqrt{z}) dz \right] \right). \end{aligned} \quad (14)$$

Finally, the unconditioned ASEP under coordinated frequency reuse is expressed as

$$\begin{aligned} ASEP_{\text{IM}} = & w_1 \left(1 - \int_0^\infty \mathcal{U}(z) \frac{e^{-z}}{\sqrt{\pi z}} dz \right) \\ & + w_2 \left(1 - 2 \int_0^\infty \mathcal{U}(z) \frac{e^{-z} \text{erfc}(\sqrt{z})}{\sqrt{\pi z}} dz \right), \end{aligned} \quad (15)$$

such that $\mathcal{U}(z)$ is given in (13).

As shown in (15), the interference protection imposed by the coordinated frequency reuse scheme highly complicates the ASEP expression. Nevertheless, the integrals in (15) can be numerically evaluated by Matlab and the results can be used to draw design insights. For the BS coordination only (i.e., without frequency reuse), the exact ASEP is similar to the expression given in (15) without the intensity thinning factor Δ^{-1} in the first term in the exponent of (13).

It is worth noting that, when comparing the results in [17, equation (10)] to the proposed baseline model in (9), one can see that the EiD approach yields complex double-integral ASEP expressions whose computational complexity and runtime are huge due to the sum of the hypergeometric functions in the exponent. This renders the analysis of more

complicated scenarios, such as the coordinated frequency reuse scheme, infeasible.

IV. SIMULATION RESULTS

In this section, we verify the proposed analysis, for the depicted downlink scenario, via Monte Carlo simulations and against the EiD approach, which is denoted as “*Exact*” in the figures. We vary the BS transmit powers P , while keeping N_o constant. Unless otherwise stated, the path-loss exponent $\eta = 4$, the noise power $N_o = -90$ dBm, the users intensity $\lambda_u = 30$ UEs/km², the BSs intensity $\lambda = 10$ BSs/km², Rayleigh fading is assumed with unity mean channel (power) gain. The desired and interfering symbols are modulated using square quadrature amplitude modulation (QAM) scheme, with a constellation size $M \in \{4, 16\}$. For illustration purposes, we consider the intended and the interfering signals to be modulated via the same modulation scheme.

Figs. 1 and 2 quantify the performance of the ASEP under coordinated frequency reuse for different values of Δ , for 4-QAM and 16-QAM modulated signals, respectively. The figures show a close match between simulations and the proposed Gaussian codebook approximation for all values of Δ , which validates our analysis. We also plot the EiD approach, which is denoted as “*Exact*” in the figures, for $\Delta = 1$ case to demonstrate that the exact EiD analysis highly matches the proposed analysis. Extensions of the EiD approach for higher values of Δ are not investigated due to tractability issues.

In Figs. 1 and 2, we plot the aggressive frequency reuse scheme ($\Delta = 1$) and the noise-limited downlink performance to benchmark the frequency reuse performance. The performance gap between the noise-limited and the derived expressions for the ASEP represents the performance degradation of the MLR due to aggregate network interference. Hence, the figures clearly show the penalty of interference. That is, while the ASEP in the noise-limited case monotonically decreases with the transmitted power, the ASEP in downlink network saturates at a certain power, due to the transition to the interference-limited operation. This saturation is due to the fact that the noise term becomes negligible as P increases and therefore the increase in the serving BS transmit power is canceled by the increase in interference signals. No matter how much interferers are avoided with coordinated frequency reuse, the ASEP performance will be interference-limited at a certain transmit power. However, the transition point from the noise-limited operation to the interference-limited operation depends on the frequency reuse scheme. The figures also show the additional gain acquired by increasing Δ . It is worth noting that these results may be exploited to design the transmit power of the cellular network such that a noise-limited operation is always guaranteed. This is because any

$$\mathcal{L}_{\tilde{X}|\|x_o\|}(s) = \exp \left\{ -\frac{2(\pi\lambda)^{\Delta+1} \|x_o\|^{2\Delta}}{\Delta\Gamma(\Delta-1)} \int_1^\infty r(r^2-1)^{\Delta-2} e^{-\pi\lambda\|x_o\|^2(r^2-1)} \sqrt{s} \arctan\left(\frac{\sqrt{s}}{r^2}\right) dr \right\}. \quad (12)$$

$$\mathcal{U}(z) = \int_0^\infty 2\pi\lambda x \exp \left\{ -\frac{2(\pi\lambda)^{\Delta+1} x^{2\Delta}}{\Delta\Gamma(\Delta-1)} \int_1^\infty r(r^2-1)^{\Delta-2} e^{-\pi\lambda x^2(r^2-1)} \sqrt{s} \arctan\left(\frac{\sqrt{s}}{r^2}\right) dr - \pi\lambda x^2 - \frac{zN_o x^4}{\beta P} \right\} dx. \quad (13)$$

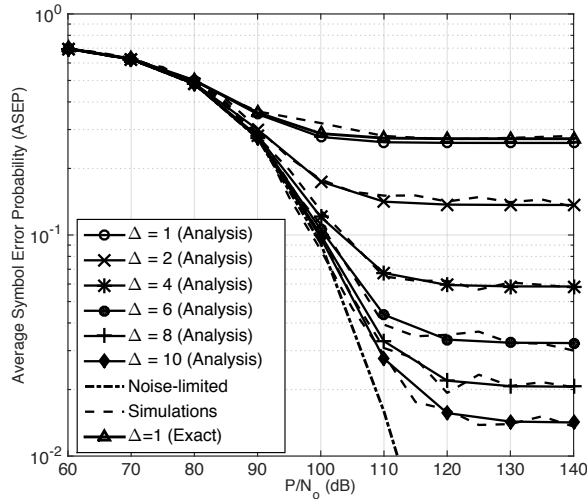


Fig. 1. The effect of coordinated frequency reuse on the average symbol error probability in the downlink scenario for 4-QAM modulated signals.

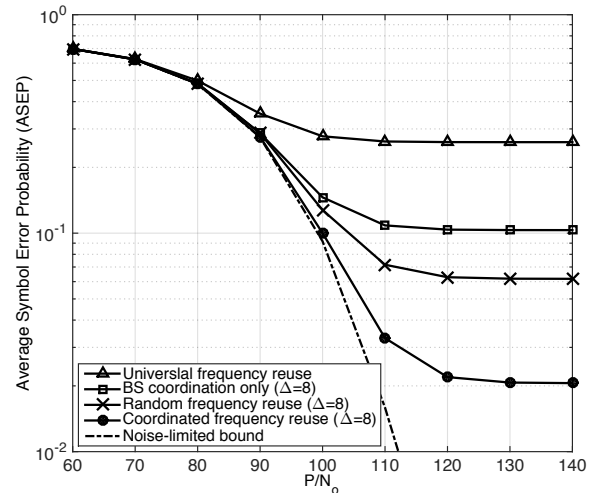


Fig. 3. The effect of coordination and frequency reuse on average symbol error probability in the downlink scenario for 4-QAM modulated signals.

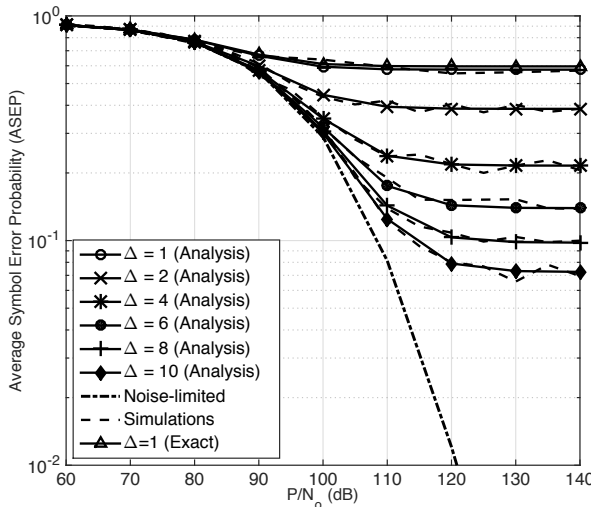


Fig. 2. The effect of coordinated frequency reuse on the average symbol error probability in the downlink scenario for 16-QAM modulated signals.

increase in the transmit power after the transition to the interference-limited operation is wasted.

In Fig. 3, the impact of the different interference management techniques, namely, BSs coordination, random frequency reuse, and coordinated frequency reuse on the ASEP performance improvement is investigated. The figure also shows the degraded ASEP performance due to the aggressive frequency reuse for $\Delta = 1$. Hence, interference manage-

ment is essential for adequate network operation. While it is obvious that the coordinated frequency reuse scheme achieves the best ASEP performance, it is not intuitive that the random frequency reuse scheme outperforms the BS coordination. Hence, it can be concluded that the interferers intensity have more prominent effect than the interference boundaries in cellular networks. This is because the UEs are already protected in the downlink via the association strategy from arbitrary nearby interferers. The figure also shows that coordinated frequency reuse provides an additional 35% and 80% reduction in the ASEP over, respectively, the random frequency reuse, and BS coordination.

V. CONCLUSION

In this paper, we analyze the average symbol error performance with interference management in downlink cellular networks, through a simple unified framework. The proposed approach characterizes the parametric ASEP in realistic interference environments and captures several key network parameters. Though approximate, the presented analysis yields simple single-integral ASEP expressions while maintaining the accuracy and generality of the exact EiD approach. We investigate different interference management techniques for the purpose of enhancing the ASEP performance. We observe that coordinated frequency reuse provides 35% lower ASEP than the random frequency reuse. Also, we show that random frequency reuse outperforms BSs coordination only by up to 40% lower ASEP.

APPENDIX A
PROOF OF LEMMA 1

Since the number of points in disjoint regions are independent, the conditional CDF for the distance to the n^{th} neighboring BS can be written as

$$\mathbb{P}\{\|x_n\| < r \mid \|x_o\| = r_o\} = 1 - \sum_{k=0}^{n-1} \frac{\pi\lambda(r^2 - r_o^2)^k e^{-\pi\lambda(r^2 - r_o^2)}}{k!}. \quad (16)$$

By differentiating (16), the conditional PDF is given by

$$f_{\|x_n\| \mid \|x_o\|}(r \mid \|x_o\| = r_o) = 2\pi\lambda r e^{-\pi\lambda(r^2 - r_o^2)} \left(\sum_{k=0}^{n-1} \frac{\pi\lambda(r^2 - r_o^2)^k}{k!} - \mathbb{1}_{\{n>2\}} \sum_{k=0}^{n-2} \frac{\pi\lambda(r^2 - r_o^2)^k}{k!} \right) \quad (17)$$

which can be further simplified to the form of (10). Then, multiplying (10) by the PDF of $\|x_o\|$, the joint PDF of $\|x_n\|$ and $\|x_o\|$ is given as in (11).

APPENDIX B
PROOF OF LEMMA 2

Let $n = \Delta - 1$. Since the distance of the interferers $\|x_i\| > \|x_n\|$, then the LT of the residual conditional interference is obtained from

$$\begin{aligned} \mathcal{L}_{\tilde{X}}(s) &= \mathbb{E} \left[\prod_{i \in \tilde{\Psi} \setminus \mathcal{I}_\Delta} e^{-s \frac{\|x_i\|^{-\eta} g_i}{\|x_o\|^{-\eta}} \right] \\ &\stackrel{(a)}{=} \exp \left\{ -2\pi\lambda \int_{\|x_n\|}^{\infty} \mathbb{E} \left[1 - e^{-s \frac{\|x\|^{-\eta} g}{\|x_o\|^{-\eta}} \right] x dx \right\} \\ &\stackrel{(b)}{=} \exp \left\{ \frac{-2\pi\lambda}{\eta} \|x_n\|^2 \int_0^1 \left[1 - \left(\frac{m}{m + sy \frac{\|x_o\|^\eta}{\|x_n\|^\eta}} \right)^m \right] \frac{1}{y^{\frac{2}{\eta} + 1}} dy \right\} \\ &\stackrel{(c)}{=} \exp \left\{ -\pi\lambda \|x_n\|^2 \left[{}_2F_1 \left(\frac{-2}{\eta}, m; 1 - \frac{2}{\eta}; -s \frac{\|x_o\|^\eta}{m \|x_n\|^\eta} \right) - 1 \right] \right\} \\ &\stackrel{(\eta=4, m=1)}{=} \exp \left\{ -\pi\lambda \|x_o\|^2 \sqrt{s} \arctan \left(\sqrt{s} \frac{\|x_o\|^2}{\|x_n\|^2} \right) \right\}, \quad (18) \end{aligned}$$

where (a) is obtained by utilizing the PGFL of the interfering PPP $\tilde{\Psi}$ [20], (b) follows from the LT of the gamma distribution of g with parameter m , with a simple change of variables $y = \frac{\|x_n\|^\eta}{x^\eta}$ and (c) is obtained by solving the integral using [25] where ${}_2F_1(a, b; c; z) = \sum_{k=0}^{\infty} \frac{(a)_k (b)_k}{(c)_k k!} z^k$ is the Gauss hypergeometric function [22]. Then, we average over the conditional distribution of $\|x_n\|$ given $\|x_o\|$, and apply the change of variables $r = \frac{\|x_n\|}{\|x_o\|}$ to get (13).

REFERENCES

- [1] L. H. Afify, H. ElSawy, T. Y. Al-Naffouri, and M.-S. Alouini, "On average symbol error performance in cellular networks: A stochastic geometry approach," submitted to a journal publication.
- [2] J. G. Andrews, F. Baccelli, and R. K. Ganti, "A tractable approach to coverage and rate in cellular networks," *IEEE Trans. Commun.*, vol. 59, no. 11, pp. 3122–3134, Nov. 2011.
- [3] H. S. Dhillon, R. K. Ganti, F. Baccelli, and J. G. Andrews, "Coverage and ergodic rate in k-tier downlink heterogeneous cellular networks," in *Communication, Control, and Computing (Allerton), 2011 49th Annual Allerton Conference on*, Sept. 2011, pp. 1627–1632.
- [4] A. Guo and M. Haenggi, "Spatial stochastic models and metrics for the structure of base stations in cellular networks," *IEEE Trans. Wireless Commun.*, vol. 12, no. 11, pp. 5800–5812, Nov. 2013.

- [5] H. ElSawy, E. Hossain, and M. Haenggi, "Stochastic geometry for modeling, analysis, and design of multi-tier and cognitive cellular wireless networks: A survey," *IEEE Commun. Surveys Tuts.*, vol. 15, no. 3, pp. 996–1019, 2013.
- [6] H. ElSawy and E. Hossain, "On stochastic geometry modeling of cellular uplink transmission with truncated channel inversion power control," *IEEE Trans. Wireless Commun.*, vol. 13, no. 8, pp. 4454–4469, Aug. 2014.
- [7] H.S. Dhillon, R.K. Ganti, and J.G. Andrews, "Load-aware heterogeneous cellular networks: Modeling and sir distribution," in *Global Communications Conference (GLOBECOM), 2012 IEEE*, Dec 2012, pp. 4314–4319.
- [8] H.S. Dhillon, T.D. Novlan, and J.G. Andrews, "Coverage probability of uplink cellular networks," in *Global Communications Conference (GLOBECOM), 2012 IEEE*, Dec 2012, pp. 2179–2184.
- [9] H. ElSawy and E. Hossain, "Two-tier HetNets with cognitive femto-cells: Downlink performance modeling and analysis in a multichannel environment," *IEEE Trans. Mobile Comput.*, vol. 13, no. 3, pp. 649–663, Mar. 2014.
- [10] S. Govindasamy, D. W. Bliss, and D. H. Staelin, "Asymptotic spectral efficiency of the uplink in spatially distributed wireless networks with multi-antenna base stations," *IEEE Trans. Commun.*, vol. 61, no. 7, pp. 100–112, July 2013.
- [11] H.S. Dhillon, M. Kountouris, and J.G. Andrews, "Downlink mimo het-nets: Modeling, ordering results and performance analysis," *Wireless Communications, IEEE Transactions on*, vol. 12, no. 10, pp. 5208–5222, October 2013.
- [12] A.K. Gupta, H.S. Dhillon, S. Vishwanath, and J.G. Andrews, "Downlink coverage probability in mimo hetnets with flexible cell selection," in *Global Communications Conference (GLOBECOM), 2014 IEEE*, Dec 2014, pp. 1534–1539.
- [13] Xincheng Zhang and M. Haenggi, "Successive interference cancellation in downlink heterogeneous cellular networks," in *Globecom Workshops (GC Wkshps), 2013 IEEE*, Dec 2013, pp. 730–735.
- [14] G. Nigam, P. Minero, and M. Haenggi, "Coordinated multipoint joint transmission in heterogeneous networks," *Communications, IEEE Transactions on*, vol. 62, no. 11, pp. 4134–4146, Nov 2014.
- [15] A.H. Sakr and E. Hossain, "Location-aware cross-tier coordinated multipoint transmission in two-tier cellular networks," *Wireless Communications, IEEE Transactions on*, vol. 13, no. 11, pp. 6311–6325, Nov 2014.
- [16] M. K. Simon and M.-S. Alouini, *Digital Communication over Fading Channels*, vol. 95, Wiley-Interscience, 2005.
- [17] M. Di Renzo and W. Lu, "The equivalent-in-distribution (EiD)-based approach: On the analysis of cellular networks using stochastic geometry," *IEEE Commun. Lett.*, vol. 18, no. 5, pp. 761–764, May 2014.
- [18] P. C. Pinto and M. Z. Win, "Communication in a poisson field of interferers—Part I: Interference distribution and error probability," *IEEE Trans. Wireless Commun.*, vol. 9, no. 7, pp. 2176–2186, July 2010.
- [19] Y. M. Shobowale and K. A. Hamdi, "A unified model for interference analysis in unlicensed frequency bands," *IEEE Trans. Wireless Commun.*, vol. 8, no. 8, pp. 4004–4013, Aug. 2009.
- [20] M. Haenggi, *Stochastic Geometry for Wireless Networks*, Cambridge University Press, 2012.
- [21] K. A. Hamdi, "A useful technique for interference analysis in nakagami fading," *IEEE Trans. Wireless Commun.*, vol. 55, no. 6, pp. 1120–1124, June 2007.
- [22] M. Abramowitz and I. A. Stegun, Eds., *Handbook of Mathematical Functions, Tenth Printing*, Dover Publications, Dec. 1972.
- [23] M. Haenggi, "Mean Interference in Hard-Core Wireless Networks," *IEEE Communications Letters*, vol. 15, no. 8, pp. 792–794, Aug. 2011, Available at <http://www.nd.edu/~mhaenggi/pubs/c11.pdf>.
- [24] H.Q. Nguyen, F. Baccelli, and D. Kofman, "A stochastic geometry analysis of dense IEEE 802.11 networks," in *In Proc. of the 26th IEEE International Conference on Computer Communications, INFOCOM 2007.*, May 2007, pp. 1199–1207.
- [25] I. S. Gradshteyn and I. M. Ryzhik, *Table of Integrals, Series, and Products, Seventh Edition*, Academic Press, 2007.